

Planar Archimedean Spiral Antenna Resonant Frequency and Bandwidth Estimation using MLP Neural Network

Zoran Stanković, *Member, IEEE*, Maja Sarevska, Nebojša Dončov, *Senior Member, IEEE*, Ksenija Pešić

Abstract— This paper presents a neural model for fast estimation of the resonant frequency and bandwidth of a planar Archimedean spiral antenna based on MultiLayer Perceptron (MLP) network. The input parameters of the model are the number of turns of the spiral, the inner radius of the spiral and the outer radius of the spiral, while the output parameters of the model are resonant frequency, minimum operating frequency and maximum operating frequency of the Archimedean spiral antenna. The proposed neural model was applied in the process of modeling a planar self-complementary Archimedean spiral antenna with two arms.

Index Terms— Archimedean spiral antenna, neural network, neural model.

I. INTRODUCTION

Planar Archimedean spiral antennas, due to their low weight, simplicity of construction, low manufacturing cost and approximately frequency-independent characteristics in a wide frequency range, have significant applications in broadband communication systems (*Ultra-Wide Band (UWB)* communication systems, satellite communication systems, ground penetrating radars, military aircraft radars and other broadband systems) [1],[2].

The classic approach in the analysis of characteristics, modeling and design of such antenna structures is the use of EM simulators based on numerical EM modeling techniques such as Method of Moments (MoM), Finite Element Method (FEM), Transmission Line Matrix (TLM) method, Finite Difference Time Domain (FDTD) and others [3],[4]. The main disadvantages of this approach are the need for strong hardware resources and long computation times.

An alternative approach that can overcome the above problems is the use of artificial neural networks to model planar spiral antennas. For this purpose, a good candidate in

Zoran Stanković is with the Faculty of Electronic Engineering, University of Niš, A. Medvedeva 14, 18000 Niš, Serbia (e-mail: zoran.stankovic@elfak.ni.ac.rs).

Maja Sarevska is with American University of Europe-FON, str. Kiro Gligorov bb, 1000 Skopje, North Macedonia (e-mail: maja.sarevska@fon.edu.mk).

Nebojša Dončov is with the Faculty of Electronic Engineering, University of Niš, A. Medvedeva 14, 18000 Niš, Serbia (e-mail: nebojsa.doncov@elfak.ni.ac.rs).

Ksenija Pešić is with the Faculty of Electronic Engineering, University of Niš, A. Medvedeva 14, 18000 Niš, Serbia (e-mail: ksenija.pesic@elfak.ni.ac.rs)

the modeling process is the MultiLayer Perceptron (MLP) network [5],[6], which has shown good results in modeling planar antenna structures [7],[8].

As part of the research covered by this paper, the "ASA_design_MT software" was first implemented for the analysis of the characteristics and design of the planar Archimedean spiral antenna with two arms. Then, a neural model of this antenna was developed, which is based on the MLP network and which is presented in this paper. Data generated by ASA_design_MT software was used to develop this model.

II. PLANAR ARCHIMEDEAN SPIRAL ANTENNA

The architecture of the planar Archimedean spiral antenna with two arms is shown in Figure 1. The basic geometric parameters of the antenna are: inner radius of the spiral antenna r_i , outer radius of the spiral antenna r_o , arm width w , space between arms s , and feed point f .

The Archimedean spiral curve is determined by the equation

$$r = a\theta + r_i \quad (1)$$

where r is the radius of curve, a is the growth rate, θ is the winding angle, and r_i is the inner radius of spiral [2]. Accordingly, the outer radius of the spiral is defined in a way

$$r_o = 2\pi ta + r_i \quad (2)$$

where t is the number of spiral turns. Two edge curves of c_1 and c_2 describe one spiral arm as

$$\begin{aligned} c_1 &= a\theta + r_i \\ c_2 &= a(\theta + \theta_{off}) + r_i \end{aligned} \quad (3)$$

where θ_{off} is the offset angle. The metal (arm) width w and the metallization ratio χ of spiral antenna can then be defined as [2]

$$\begin{aligned} w &= |c_1 - c_2| = a\theta_{off} \\ \chi &= \frac{w}{w + s} = \frac{\theta_{off}}{\pi} \end{aligned} \quad (4)$$

In this paper, the case where the Archimedean spiral antenna is a self-complementary antenna is considered. This case is obtained when the condition $w = s$ is met. In this case

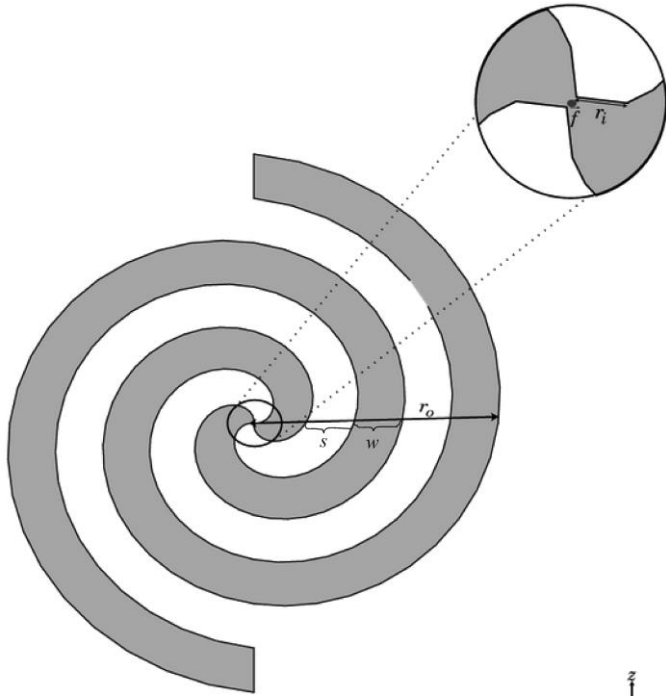


Fig. 1. Architecture of the planar Archimedean spiral antenna with two arms (r_i - inner radius of the spiral antenna, r_o - outer radius of the spiral antenna, w - arm width, s - space between arms, f - feed point).

the metallization ratio, offset angle, growth rate and arm width can be determined by equations

$$\begin{cases} \chi = \frac{1}{2} \\ \theta_{off} = \frac{\pi}{2} \\ a = \frac{2w}{\pi} \\ w = \frac{r_o - r_i}{4t} \end{cases} \quad (5)$$

By applying Babinet's principle [1]

$$z_{metal} z_{air} = \frac{\eta_0^2}{4} \quad (6)$$

where η_0 is the characteristic impedance of free space, to an ideal planar self-complementary Archimedean spiral antenna ($r_i \rightarrow 0$, $r_o \rightarrow \infty$), the input impedance of the antenna can be calculated [1]

$$z_{in} = \frac{\eta_0}{2} \approx 188 \Omega \quad (7)$$

In this case the antenna has infinite bandwidth and all primary characteristics (input impedance, antenna efficiency) and secondary characteristics of the antenna (radiation characteristics, directivity, polarization) are frequency independent. If the planar self-complementary Archimedean spiral antenna has limited physical dimensions then its bandwidth is wide but limited and its impedance deviates to

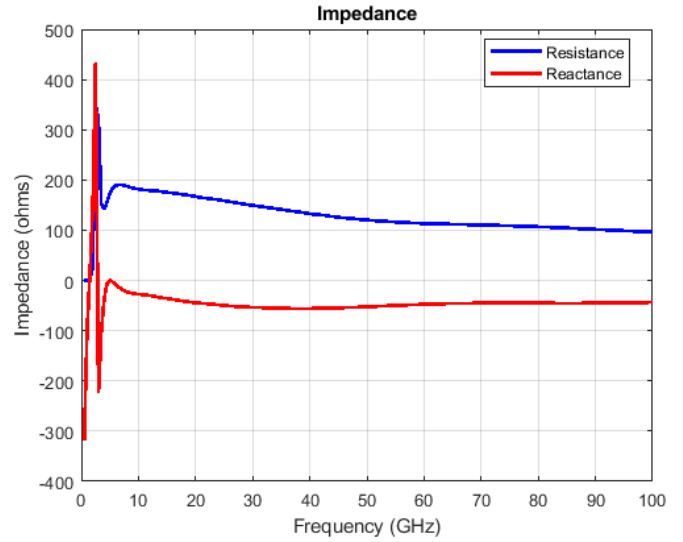


Fig 2. Impedance of the planar self-complementary ASA vs frequency ($t = 1$, $r_i = 2$ mm $r_o = 2$ cm)

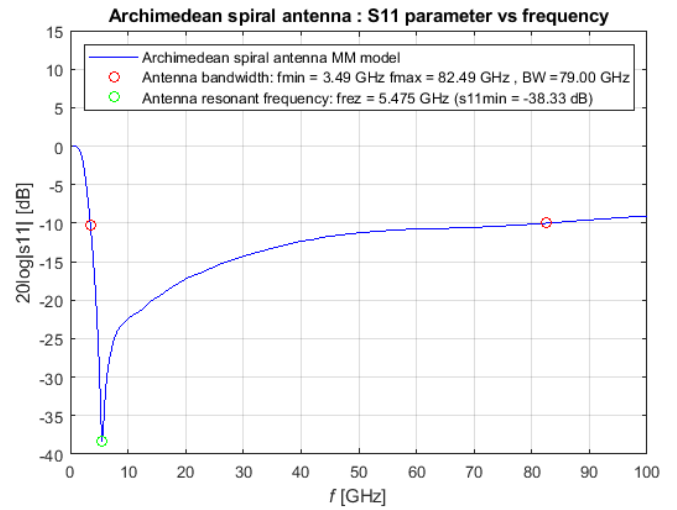


Fig. 3. S_{11} parameters of the planar self-complementary ASA vs frequency ($t = 1$, $r_i = 2$ mm $r_o = 2$ cm)

some extent from 188Ω . In this case, the approximate theoretical formula for determining the lower bound of bandwidth is [1]

$$f_{min} = \frac{c}{2\pi r_o} \quad (8)$$

In practice, the lower bound of bandwidth will be greater than predicted by Eq.8 due to reflections from the end of the arm.

If the antenna does not use a tapered feed region in the spiral center, the upper bound of bandwidth can be determined by the approximate theoretical formula [1]

$$f_{max} = \frac{c}{2\pi r_i} \quad (9)$$

In practice, the upper bound of bandwidth differs from the theoretical value due to the influence of the real physical geometry of the feed region.

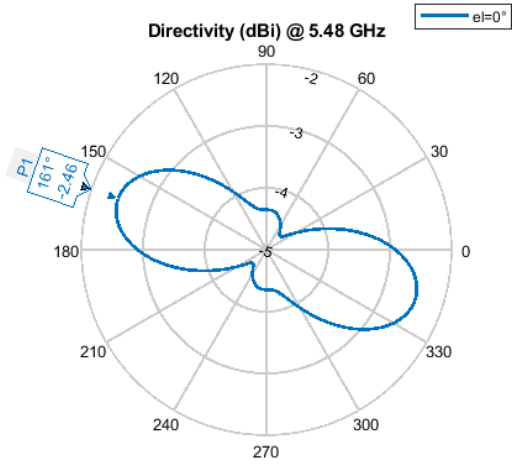


Fig. 4. Directivity of the planar self-complementary ASA in the azimuthal plane at $f_r = 5.475$ GHz ($t = 1$, $r_i = 2$ mm $r_o = 2$ cm)

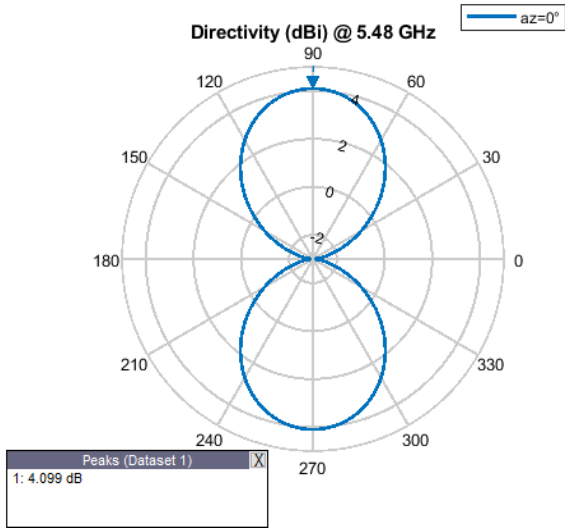


Fig. 5. Directivity of the planar self-complementary ASA in the elevation plane at $f_r = 5.475$ GHz ($t = 1$, $r_i = 2$ mm $r_o = 2$ cm)

III. EM MODELING OF A PLANAR ASA USING “ASA_DESIGN_MT” SOFTWARE

In order to perform EM analysis and modeling of primary and secondary characteristics of the planar self-complementary Archimedean spiral antenna (ASA), “ASA_design_MT” software was developed. This software is based on Method of Moments (MoM) and is implemented using the MATLAB Antenna toolbox.

Figures 2 and 3 show the impedance and s_{11} parameter as a function of frequency for a planar self-complementary ASA with physical parameters $t = 1$, $r_i = 2$ mm and $r_o = 2$ cm. It can be seen that the antenna at the resonant frequency $f_r = 5.475$ GHz has a resistance of 188 Ω . As the frequency increases, the impedance takes on a slightly capacitive character, while the resistance slowly decreases compared to 188 Ω .

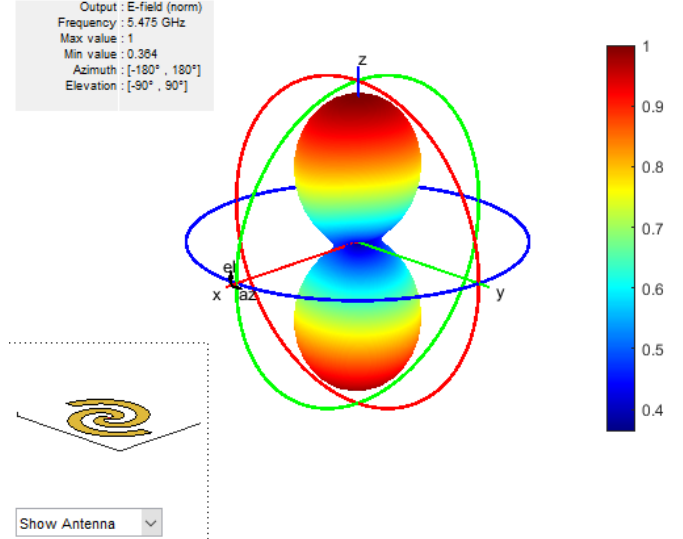


Fig. 6. 3D radiation pattern of the planar self-complementary ASA at $f_r = 5.475$ GHz ($t = 1$, $r_i = 2$ mm $r_o = 2$ cm)

Figures 4, 5 and 6 show the directivity of the planar self-complementary ASA in the azimuthal plane, the directivity of the planar self-complementary ASA in the elevation plane and the 3D radiation pattern of the planar self-complementary ASA at resonant frequency, respectively.

IV. MLP MODEL OF THE PLANAR SELF-COMPLEMENTARY ASA

The MLP model of the planar self-complementary ASA (MLP_ASA) consists of a single MLP network and its architecture is shown in Figure 7. MLP_ASA models the dependence of lower bound of bandwidth, resonant frequency and upper bound of bandwidth on the following physical parameters: number of spiral turns, inner radius of spiral and outer radius of spiral. Therefore, MLP_ASA can be functionally described by the following expression

$$[f_{\min} \ f_r \ f_{\max}]^T = f_{MLP_ASA}([t \ r_i \ r_o]^T) \quad (10)$$

MLP networks consist of a single input layer, a single output layer, and multiple hidden layers of neurons. In accordance with Eq. 10, the input layer has three neurons, the output layer has three neurons, while the hidden layers have N_1, N_2, \dots, N_H neurons respectively, where H is the total number of hidden layers. For MLP network with a specific number of layers and neurons in them, notation was used $MLPH-N_1 \dots -N_H$, $1 \leq i \leq H$.

The outputs of the hidden layers are given by the expression

$$\mathbf{y}_l = F(\mathbf{w}_l \mathbf{y}_{l-1} + \mathbf{b}_l) \quad l = 1, 2, \dots, H \quad (11)$$

where \mathbf{y}_0 represents the output of the input layer and vectors \mathbf{y}_l and \mathbf{y}_{l-1} represent the output of l -th and $(l-1)$ -th hidden layer, respectively. Weight matrix for connections between neurons in $(l-1)$ -th and l -th layers is denoted by \mathbf{w}_l , while biases of l -th hidden layer neurons are represented by vector \mathbf{b}_l . Neurons in

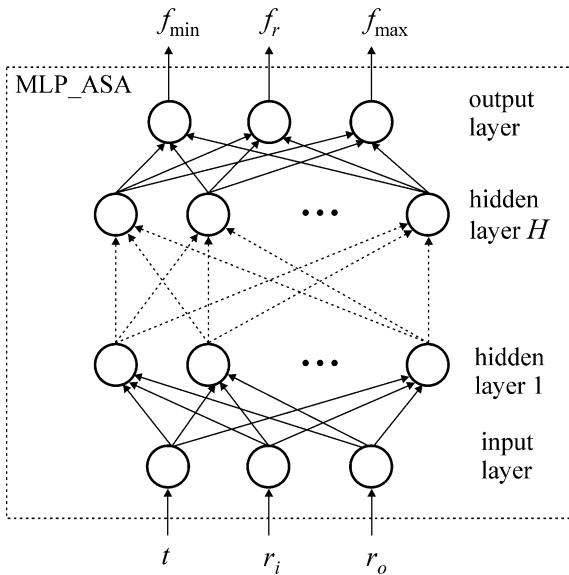


Fig. 7. The MLP neural model of the planar self-complementary Archimedean spiral antenna

hidden layers have the hyperbolic tangent sigmoid activation function $F(\cdot)$ defined by the expression

$$F(u) = \frac{e^u - e^{-u}}{e^u + e^{-u}} \quad (12)$$

The neurons in the output layer use a linear activation function so that their output is defined in a way

$$\begin{bmatrix} f_{\min} & f_r & f_{\max} \end{bmatrix}^T = \mathbf{w}_{H+1} \mathbf{y}_H + \mathbf{b}_{H+1} \quad (13)$$

where \mathbf{w}_{H+1} is a weight matrix for connections between neurons of the last hidden layer and output layer neurons.

During the training of the MLP network, the weight matrices $\mathbf{w}_1, \mathbf{w}_2, \dots, \mathbf{w}_H, \mathbf{w}_{H+1}$ and bias vectors $\mathbf{b}_1, \mathbf{b}_2, \dots, \mathbf{b}_H, \mathbf{b}_{H+1}$ are optimized in order to achieve the desired mapping accuracy defined by the expression Eq. 10.

V. MODELING RESULTS

Using the “ASA_design_MT” software 1000 samples are generated for training and 300 samples for testing having random distribution.

With the aim to develop a model with better accuracy the training was done for various $MLPH-N_1 \dots -N_r \dots -N_H$ networks while only networks with two hidden layers were used ($H = 2$). For the number of neurons in the hidden layer, the values that were used are $6 \leq N_1, N_2 \leq 22$.

The MLP training is done using Levenberg – Marquardt algorithm with given goal mean squared error of training $MSE_{target} = 10^{-4}$ and maximal number of iterations $N_{max} = 500$. Before training the neural connection weights and biases are initialized with random values in the range [-1 1]. Also input network data are scaled and output data are descaled in the range [-1 1]. After the training each network is tested using test data in order generalization capabilities to be evaluated. For the evaluation of the generalization capabilities of the

network and its accuracy the following test metrics are used: mean squared error (RMSE) and Pearson product moment correlation coefficient (r^{PPM}) [6].

The Table I shows the testing results for eight MLP networks that showed best testing results after training. It may be seen that the networks have small RMSE in the lower bandwidth limit and resonant frequency, while in the estimation of the upper bandwidth limit they have much higher RMSE.

For the realization of the MLP model of the planar self-complementary Archimedean spiral antenna MLP2-9-8 is chosen as this network in the testing procedure had largest value for the Pearson product moment correlation coefficient.

TABLE I
TEST RESULTS FOR EIGHT MLP MODELS WITH THE HIGHEST r^{PPM} VALUE

MLP networks	RMSE (f_{\min})	RMSE (f_r)	RMSE (f_{\max})	r^{PPM}
MLP2-9-8	0.1628	0.3345	6.4747	0.9939
MLP2-10-9	0.1537	0.3628	6.4915	0.9938
MLP2-8-8	0.1584	0.3144	6.5339	0.9937
MLP2-8-11	0.1590	0.3980	6.5706	0.9937
MLP2-8-10	0.1606	0.3747	6.6170	0.9936
MLP2-11-10	0.1568	0.3223	6.5715	0.9936
MLP2-12-8	0.1569	0.3174	6.6360	0.9936
MLP2-8-15	0.1622	0.3517	6.6686	0.9935

On Fig.8 the scattering diagram of MLP2-9-8 model output is shown. It may be noticed the good match for the lower bandwidth limit and resonant frequency with the referent values. Also it may be noticed that for the values of the upper bandwidth limit the match is not so good as for the two previously mentioned parameters. This may be explained with fact that EM simulator while training sample generation had difficulty to accurately determine the upper limit of the bandwidth. The reason for that is that for higher frequencies the function of parameter s_{11} almost asymptotically approach the bound of -10 dB so the indetermination of the cross point estimation between that function and the horizontal line $s_{11} = -10$ dB is very large.

For above explained situation MLP model of the planar self-complementary ASA may be used only for rough estimation of the upper bound of the bandwidth. But this does not decrease the useful application of the proposed model because in real life the detremination of the lower bound of the bandwidth is more important than for the upper bound. The reason for this is that upper bound frequency is much higher than the maximal working frequency for emission and reception.

MLP model of the planar self-complementary ASA is implemented on a modest referent hardware platform (Intel Core i3-2350M@2.3 GHz, 4GB RAM). This model, the estimation of the resonant frequency, the minimum operating

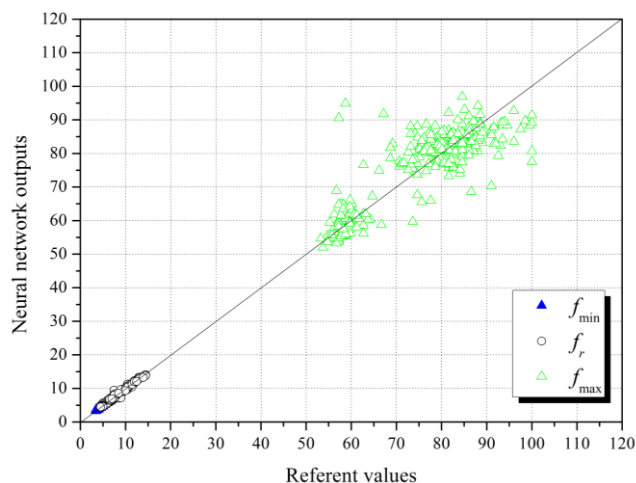


Fig. 8. Scattering diagram for MLP2-9-8 network

frequency and the maximum operating frequency of the antenna, has performed in 300 points defined with testing set for only 0.03 s. This speaks about the high speed of the MLP model.

VI. CONCLUSION

Today planar spiral antennas attract more and more attention because they are convenient for the application in the modern portable broadband communication devices. The modeling of these antenna structures with the help of EM simulators that are based on MoM techniques presents classical approach in EM characteristics modeling. Because of intensive numerical estimations this kind of EM simulators demand strong hardware platform and estimations itself may last very long, that is main disadvantage of the EM simulator approach. Alternative approach for the spiral antenna modeling is using of artificial neural networks.

This paper presents the MLP model of the planar self-complementary Archimedean spiral antenna that is implemented on a modest hardware platform. MLP model has shown exceptional speed in the estimation of resonant frequency, minimum operating frequency and maximum operating frequency for this antenna structure. Currently developed model supports estimation of the resonant frequency and minimum operation frequency with high accuracy and rough (low accuracy) estimation of high operating frequency for the antenna.

Further investigations will be steered to the increased MLP model accuracy for the planar self-complementary Archimedean spiral antenna in the maximum operating frequency estimation.

ACKNOWLEDGMENT

This work was supported by the Ministry of Education, Science and Technological Development of Republic of Serbia (Grant No. 451-03-9/2021-14/200102).

REFERENCES

- [1] Balanis, C. A., *Antenna Theory: Analysis and Design*, Wiley, New York, 2005.
- [2] Teng-Kai Chen and Gregory H. Huff, "Travelling Wave Mechanism and Novel Analysis of the Planar Archimedean Spiral Antenna in Free Space," *Progress In Electromagnetics Research*, Vol. 145, 287-298, 2014, doi:10.2528/PIER14011901.
- [3] Matthew N. O. Sadiku, *Numerical techniques in electromagnetics*, 2nd edition, CRC Press LLC, 2001.
- [4] Levent Sevgi, *Electromagnetic Modeling and Simulation*, First Edition.. The Institute of Electrical and Electronics Engineers, Inc. Published by John Wiley & Sons, Inc., 2014
- [5] S. Haykin, *Neural Networks*, New York, IEEE, 1994.
- [6] Q. J. Zhang, K. C. Gupta, *Neural networks for RF and microwave*
- [7] K. Pesic, Z. Stankovic and N. Doncov, "ANN-EM Model of Dual Band Square Patch Antenna with a Floating Rectangular Slot," 2021 15th International Conference on Advanced Technologies, Systems and Services in Telecommunications (TELSIKS), 2021, pp. 153-156, doi: 10.1109/TELSIKS52058.2021.9606409.
- [8] M. Milijić, Z. Stanković and B. Milovanović, "Efficient model of slotted patch antenna based on neural networks," *2009 9th International Conf. on Telecommunication in Modern Satellite, Cable, and Broadcasting Services*, Nis, 2009, pp. 384-387.